Available online at www.sciencedirect.com

ScienceDirect

Ceramics International 40 (2014) 3503–3509

CERAMICS INTERNATIONAL

www.elsevier.com/locate/ceramint

Oxidation protection of Ti–6Al–4V alloy using a novel glass–amorphous silica composite coating

Zunqi Xiao[a], Fatang Tan[a], Wei Wang[a], Fazhe Sun[a], Hongfei Lu[a], Xiaolin Qiu[b], Jianguo Chen[a], Xueliang Qiao[a,*]

[a]State Key Laboratory of Materials Processing and Die & Mould Technology, Huazhong University of Science and Technology, Wuhan 430074, Hubei, People's Republic of China

[b]Nanomaterials Research Center, Nanchang Institute of Technology, Nanchang 330013, Jiangxi, People's Republic of China

Received 5 August 2013; received in revised form 16 September 2013; accepted 17 September 2013
Available online 24 September 2013

Abstract

A novel glass–amorphous silica composite coating was prepared by the slurry method in order to improve the oxidation resistance of Ti–6Al–4V alloy at high temperatures. The microstructure of the as-prepared composite coating was analyzed by SEM, XRD and EDS techniques. The oxidation resistance and the microstructure evolution of the composite coating at 800 °C for 50 h were also studied. The results show that mass gains of the specimens coated with the composite coating were far less than that of the uncoated ones after oxidation of 50 h. Thick oxide scales composed of plate-like rutile TiO_2 and some granular α-Al_2O_3 formed on bare Ti–6Al–4V alloy, while quartz, cristobalite and diopside were observed in the composite coating, which are useful crystals for slowing the inward diffusion of oxygen to the substrate. The cross-sectional EDS line scanning images show that inward diffusion of oxygen and outward diffusion of Ti through the composite coating were insignificant. The microhardness profile reveals that the solid solution oxygen in Ti–6Al–4V alloy with composite coating was limited.

Keywords: D. Glass; Ti–6Al–4V alloy; Amorphous silica; Composite coating

1. Introduction

Ti alloys are usually used in the aerospace, energy industry, and military applications due to their excellent mechanical properties at elevated temperatures [1]. However, serious oxidation of Ti alloys at high temperatures limits their industrial applications owing to the formation of mixed oxides containing the less protective rutile TiO_2 and α-Al_2O_3 rather than a continuous protective α-Al_2O_3 scale during their exposure to high temperatures [2,3].

One way to increase the oxidation resistance of Ti alloys is to add alloying elements to Ti alloys [4,5]. However, addition of alloying elements may have negative effects on the mechanical properties of Ti alloys. To solve this problem, many kinds of coatings have been deposited on Ti alloys to improve their oxidation resistance without degrading their mechanical properties. For example, Xiong et al. investigated the effects of hot-dip Al–Si coating on the oxidation of TiAl-based alloy [6,7]; Gong et al. studied oxidation behavior of TiAl/TiAl+SiC gradient coatings on gamma TiAl [8]. Other methods to deposit protective coatings on Ti alloys include the ion implantation [9], thermal spray [10], pack aluminization and electrodepositing [11], sol-gel method [12,13], pack cementation [14], and magnetron sputtering [15].

In addition to the above mentioned methods for preparing protective coatings, glass and glass–ceramic materials with excellent chemical inertness and high temperature stability were also used as coatings for Ti alloys against high temperature oxidation [16–18]. At the same time, the oxidation resistance and thermal–physical properties of glass coatings at elevated temperatures can be tailored conveniently by incorporating ceramic particles into the glass matrix [19]. In previous studies, alumina particles were usually used as the ceramic particles mentioned

*Corresponding author. Tel./fax: +86 27 87541540.
E-mail address: qxlhust@gmail.com (X. Qiao).

0272-8842/$ - see front matter © 2013 Elsevier Ltd and Techna Group S.r.l. All rights reserved.
http://dx.doi.org/10.1016/j.ceramint.2013.09.079

above [20]. However, the strong tendency of interfacial reactions between alumina particles and glass matrix at high temperatures always cause the glass–alumina composite coating to be hard to be densified during pressureless sintering [21]. And this densifying process needs a higher temperature, which would cause Ti alloys to undergo serious oxidation during sintering. To solve this problem, crystalline quartz particles were considered to be suitable as they were compatible to glass matrix, and there were no serious interfacial reactions between quartz and glass during sintering [21]. Nevertheless, to the best of our knowledge, compared to crystalline quartz particles, amorphous silica particles would be more compatible to glass matrix because of their amorphous structure which is the same as that of glass matrix.

In this study, amorphous silica particles were incorporated into borosilicate glass to form a composite coating. The oxidation resistance of this composite coating on Ti–6Al–4V alloy at 800 °C was evaluated, and the microstructure evolution of the composite coating was also characterized.

2. Experimental

Ti–6Al–4V alloy specimens were prepared by cutting the rods into pieces of φ18 mm × 5 mm, grinding their surface using 1000# SiC paper and ultrasonically cleaning with ethanol.

The approximate composition of the borosilicate glass was as follows: SiO_2 35–40; B_2O_3 25–30; Al_2O_3 2–5; MgO 5–10; CaO 5–10; Na_2O 10–15 in wt%. The raw materials mixed in suitable proportions were melted at 1200 °C for about 2 h and then quenched in water to form glass frit. The frit was subsequently milled in an agate jar for about 36 h to obtain glass powders (size < 75 μm). The glass transition temperature (T_g) of the glass powders was obtained by DTA (Diamond TG/DTA, PerkinElmer Instruments). After that, a mixture of glass powders with 30 wt% amorphous silica particles was further wet ground to form a slurry. Then the slurry was brushed directly onto the surface of Ti–6Al–4V alloy, thereafter, the specimens coated with the slurry were dried and finally fired at 850 °C for 20 min to form the glass–amorphous silica composite coating.

The isothermal oxidation tests were performed at 800 °C for 50 h in static air in the muffle furnace. The specimens with and without the composite coating were cooled in air to room temperature after continuous oxidation at 800 °C for every 5 or 10 h in the muffle furnace, and then weighed using an electronic balance to study the oxidation kinetics of the specimens.

Phase analyses of the specimens before and after oxidation were done by X-ray diffraction (XRD, X'Pert PRO, PANalytical B.V., Holland). The surface morphologies and cross-sectional microstructures of the specimens were characterized by scanning electron microscopy (SEM, JSM-7600F, JEOL, Japan) with an energy dispersive X-ray spectroscopy (EDS, Inca X-Max 50, Oxford instruments Co., U.K.). And the Vickers microhardness measurement (DHV-1000) was done on the cross section of the specimens to evaluate the dissolution of oxygen in the specimens beneath the oxide scales or composite coating.

3. Results and discussion

The glass transition temperature (T_g) of the borosilicate glass was about 500 °C. According to the experiment results, the coating composed of this borosilicate glass was easy to flow away from Ti–6Al–4V substrate in oxidizing environments at 800 °C. In this study, amorphous silica particles (size < 5 μm) (Fig. 1) were incorporated into the above borosilicate glass to form the composite coating. The experiments reveal that this composite coating could be sintered well below 800 °C. However, a higher temperature is necessary to obtain a glossy composite coating which would help to improve the oxidation resistance of the coating [16]. Considering that phase transformation of Ti alloys (α to β) occurs at about 880 °C, the coating should be fired below 880 °C in order not to affect the mechanical properties of Ti alloys because the thermal expansion coefficient of Ti alloys will start a larger shift at this point. In this study, the firing temperature of the composite coating was 850 °C.

3.1. Microstructures of the as-prepared glass–amorphous silica composite coating

Fig. 2(a) shows the surface morphology of the as-prepared glass–amorphous silica composite coating. It can be seen that the composite coating had a glossy and smooth surface. Fig. 2 (b) shows the cross-sectional microstructure of the as-prepared composite coating. It can be seen that the composite coating was very uniform and showed a very good adhesion to the Ti–6Al–4V substrate. In the coating, a few pores were visible and close to spherical shape, which indicates that residual porosity could be determined by bubble formation due to the release of dissolved gas and insoluble gases entrapped in the initial pores [18]. And it can be obtained that there was no clear coating/

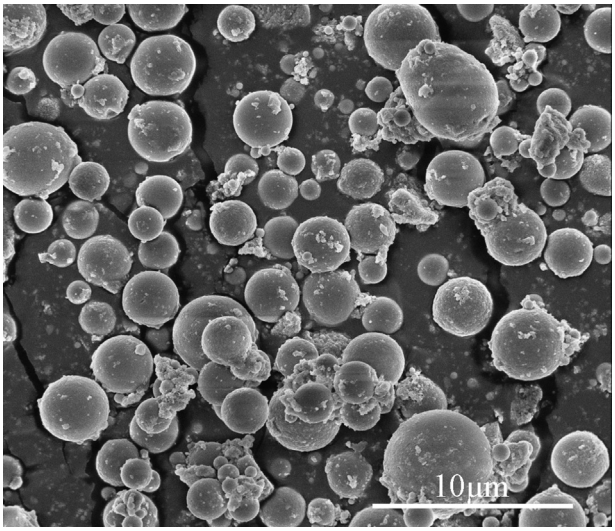

Fig. 1. SEM image of the amorphous silica.

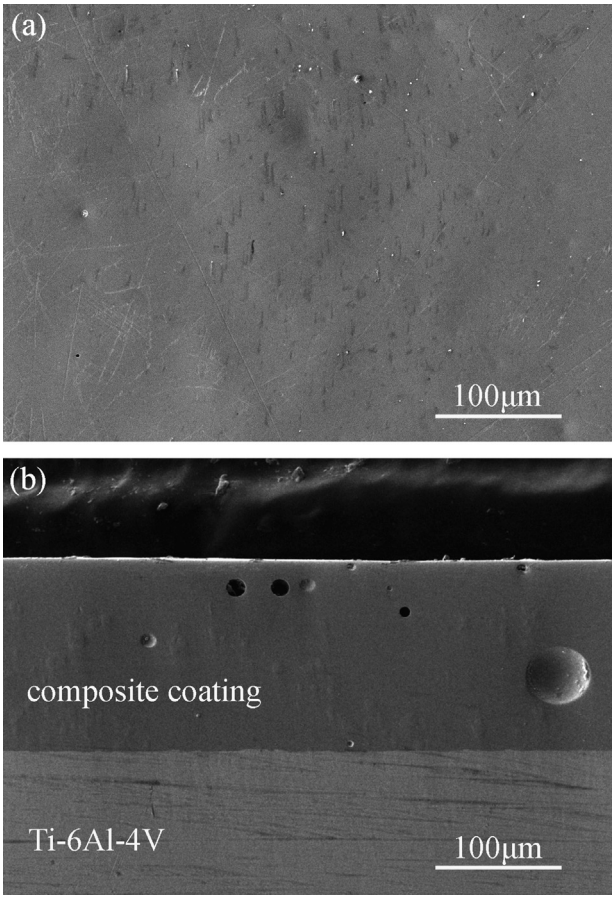

Fig. 2. SEM images of the as-prepared composite coating: (a) surface morphology and (b) cross-sectional morphology.

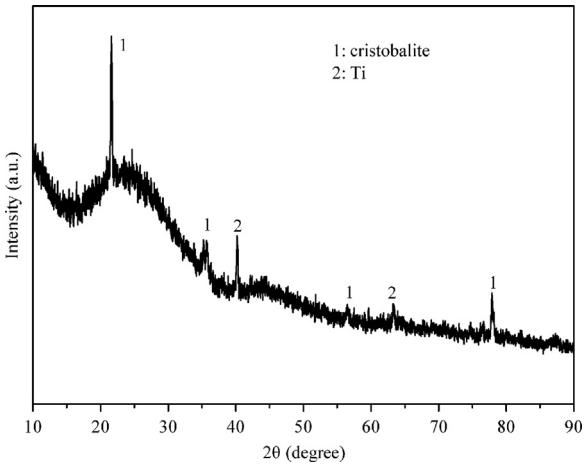

Fig. 3. XRD pattern of Ti–6Al–4V alloy with the as-prepared composite coating.

metal interface, which might be attributed to the low firing temperature of the composite coating. The XRD pattern (Fig. 3) of the coated specimen indicates that the as-prepared composite coating was composed of amorphous phase and some cristobalite crystals. The cristobalite crystals might crystallize on the surface of the amorphous silica particles, which might be attributed to the catalytic effect of the OH and O in air and in the glass network, as well as the diffusion of alkali ions from the borosilicate glass to the amorphous silica particles [22–24]. It is reported that the formation of cristobalite could increase the coefficient of thermal expansion (CET) of the composite coating, and would help to prevent the spallation of the composite coating [19,25].

3.2. Isothermal oxidation

3.2.1. Oxidation kinetics

Fig. 4 shows the isothermal oxidation kinetics of Ti–6Al–4V alloy with and without the composite coatings at 800 °C up to 50 h in air. Mass gains of bare Ti–6Al–4V alloy followed an approximately linear law, which was similar to reports of other researchers [26]. At the same oxidation condition, mass gains of the specimens coated with the composite coating were far less than those of the uncoated ones. The isothermal oxidation tests indicate that a significant improvement of the oxidation resistance of Ti–6Al–4V alloy was made by the glass–amorphous silica composite coating.

3.2.2. Microstructures of oxide scales on bare Ti–6Al–4V alloy

After isothermal oxidation of 50 h at 800 °C, bare Ti–6Al–4V alloy suffered from great oxidation with thick and spalling oxide scales. The XRD pattern of the oxide scales is shown in Fig. 5. The amplitude of the diffraction peaks of rutile TiO_2 was much higher than that of α-Al_2O_3, indicating that the oxide scales formed on bare alloy were mostly composed of rutile TiO_2.

Fig. 6(a) shows the surface morphology of bare Ti–6Al–4V alloy after 50 h oxidation. Spallation, newly formed oxide and a crack were observed on the surface of the oxide sample. The magnified image shows that the oxides of the surface were composed of plate-like TiO_2 and some granular α-Al_2O_3. Fig. 6(b) shows that a big crack formed between the thick oxide layer and Ti alloy substrate. Since the rutile TiO_2 scale is porous, brittle and poorly adherent to Ti alloy substrate, inward diffusion of oxygen and outward diffusion of Ti through oxide layer get very easy, then the oxide scales become thicker and

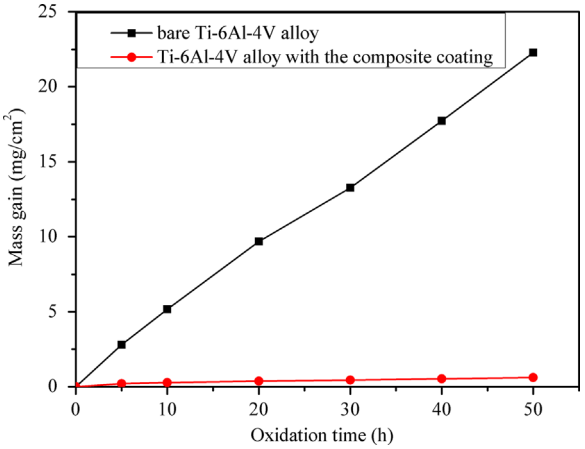

Fig. 4. Oxidation mass gains of Ti–6Al–4V alloy with and without the composite coating at 800 °C.

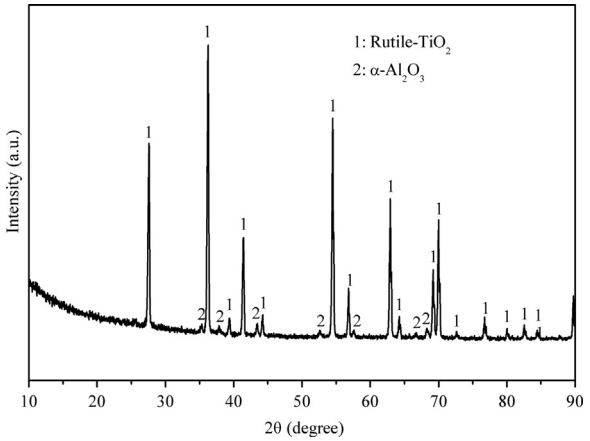

Fig. 5. XRD pattern of Ti–6Al–4V alloy after oxidation for 50 h at 800 °C.

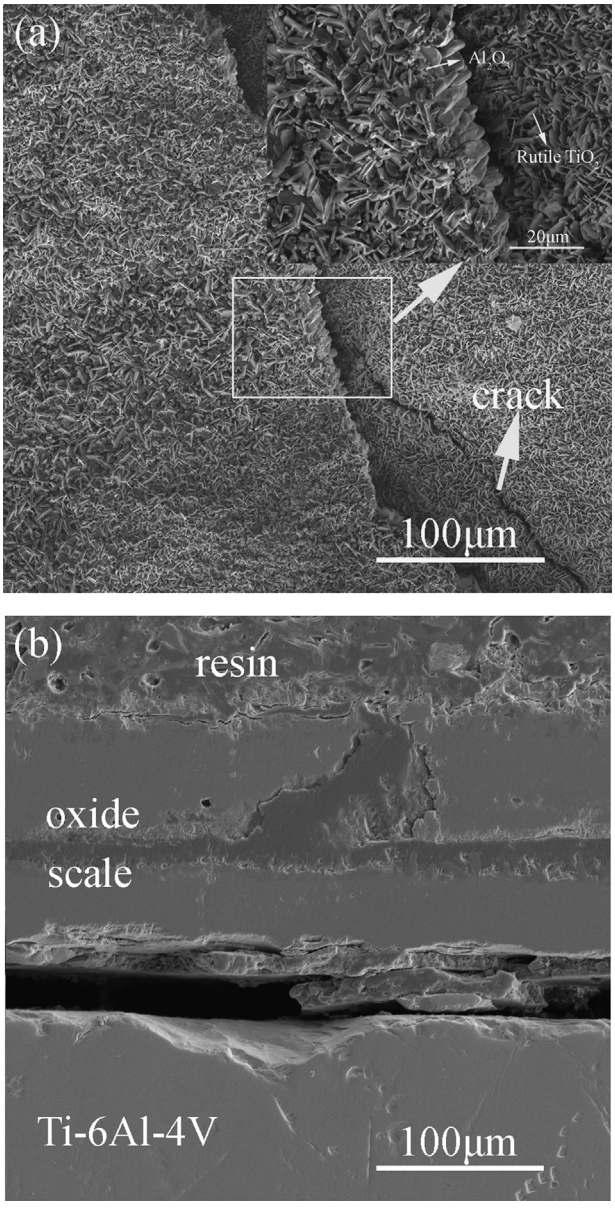

Fig. 6. SEM images of Ti–6Al–4V alloy after oxidation for 50 h at 800 °C: (a) surface morphology and (b) cross-sectional morphology.

thicker and cracks form as a result of thermal and growth stresses during the exposure to elevated temperatures [27].

3.2.3. Microstructures of the glass–amorphous silica composite coating on Ti–6Al–4V alloy after oxidation

After isothermal oxidation of 50 h at 800 °C, the composite coating still stayed on Ti–6Al–4V alloy without flowing away or spallation. In order to get a better understanding of the protection effect of the composite coating, a detailed investigation on the microstructure evolution of the composite coating was carried out.

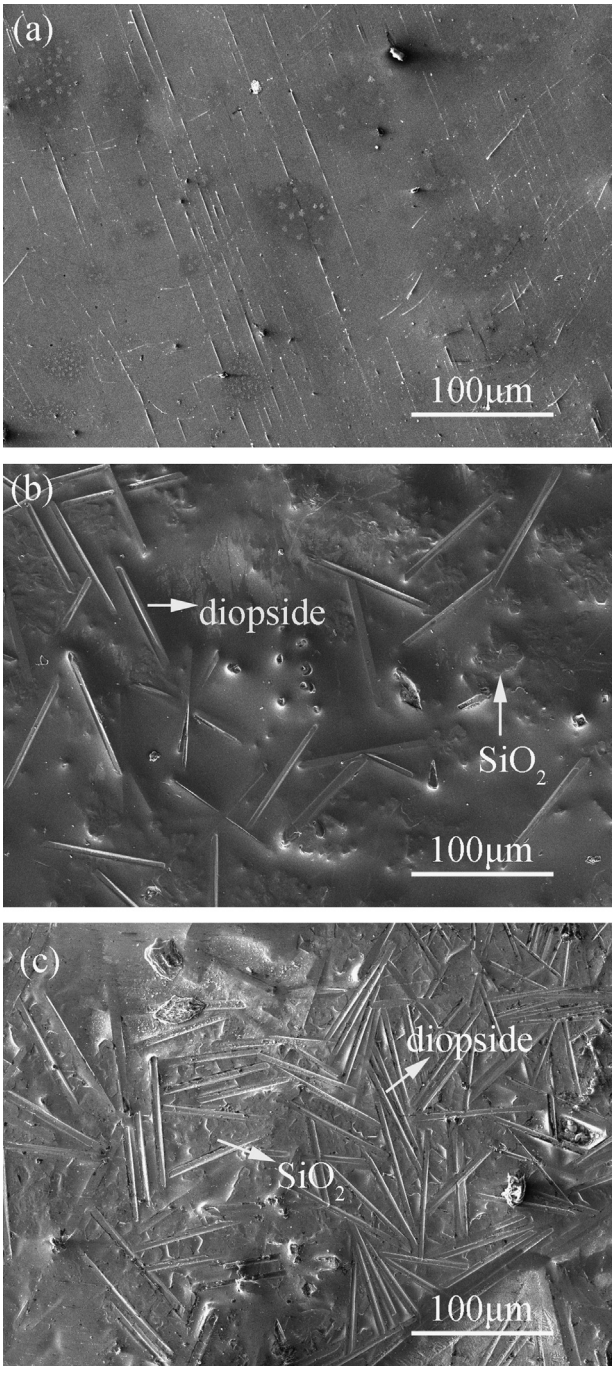

Fig. 7. SEM images of Ti–6Al–4V alloy with the composite coating after oxidation for (a) 10 h, (b) 20 h, and (c) 50 h at 800 °C.

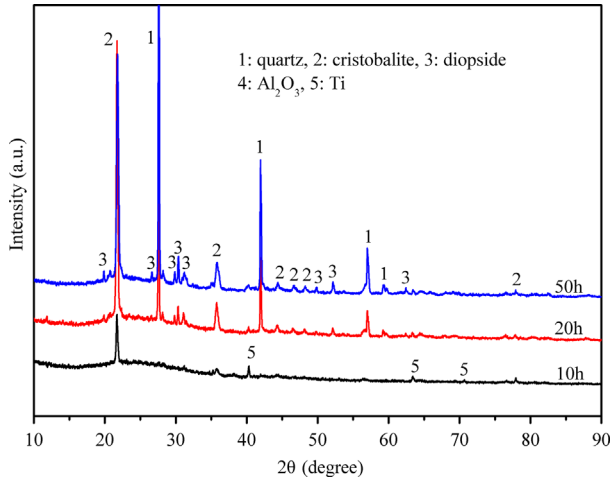

Fig. 8. XRD patterns of Ti–6Al–4V alloy with the composite coating after oxidation for 10, 20, and 50 h at 800 °C.

Figs. 7 and 8 show the surface morphologies and the XRD patterns of Ti–6Al–4V alloy with the composite coating after oxidation for 10, 20, and 50 h at 800 °C. It can be seen that after oxidation for 10 h, the composite coating still had a glossy surface and a few pores. The amplitude of the diffraction peaks of cristobalite had no apparent changes compared with the as-prepared composite coating. This implies that there were little changes in the composite coating after oxidation for 10 h. However, after oxidation for 20 h, the surface of the composite coating became rough, and some rod-shaped crystals emerged. According to the XRD and EDS analyses, it can be concluded that these rod-shaped crystals were diopside ($CaMgSi_2O_6$). The crystallization of diopside can improve the mechanical strength, corrosion resistance and thermal stability of the composite coating [28]. Apart from the diopside, the amplitude of the diffraction peaks of cristobalite became higher, implying that more cristobalite emerged. Furthermore, a mount of quartz could be seen from the XRD analysis at this time. However, it is hard to draw a clear distinction between quartz and cristobalite from the SEM and EDS analyses. In spite of this, quartz and cristobalite are useful crystals for slowing the inward diffusion of oxygen to the substrate due to the low diffusion coeffience of oxygen in SiO_2 [19]. And more diopside, cristobalite and quartz emerged after isothermal oxidation of 50 h.

Fig. 9(a) shows the coating/substrate interfacial structure after oxidation for 50 h at 800 °C. Obviously, crystals composed of diopside and SiO_2 were included in the cross-sectional microstructure of the composite coating. After isothermal oxidation of 50 h, a few spherical pores could still be seen in the composite coating. However, the coating showed an excellent adherence to the substrate without cracks or spallation. It indicates that the thermal expansion coefficient of the composite coating and the alloy substrate matched each other very well after oxidation. And it means that this composite coating would still be effective for a longer period of oxidation. According to EDS line scanning images (Fig. 9 (b)), it can be obtained that inward diffusion of oxygen and outward diffusion of Ti through the composite coating were

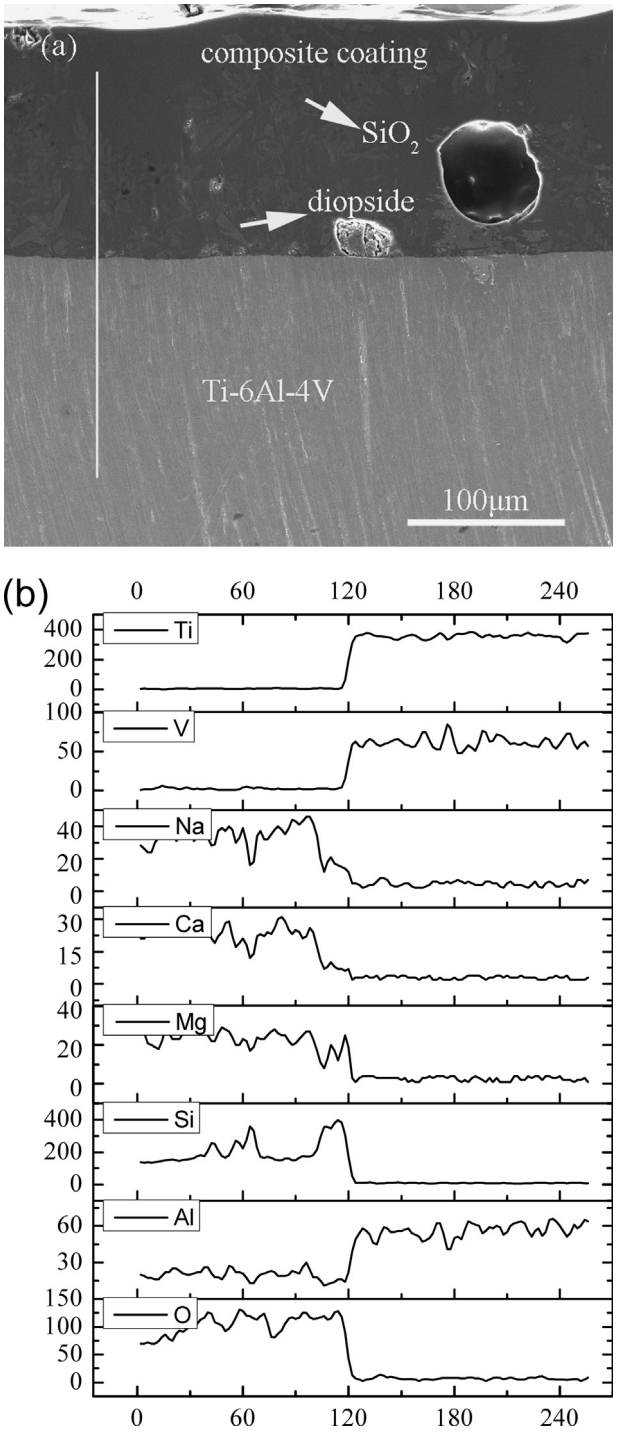

Fig. 9. Cross-sectional microstructure (a) and EDS line scanning images (b) of Ti–6Al–4V alloy with the composite coating after oxidation for 50 h at 800 °C.

insignificant. It means that the glass–amorphous silica composite coating showed good protection of Ti–6Al–4V alloy from high temperature oxidation.

3.2.4. *Microhardness profile*

The hardness of Ti alloys has much to do with the content of solid solution oxygen in the alloys, the higher content of the solid solution oxygen, the higher hardness of Ti alloys [21].

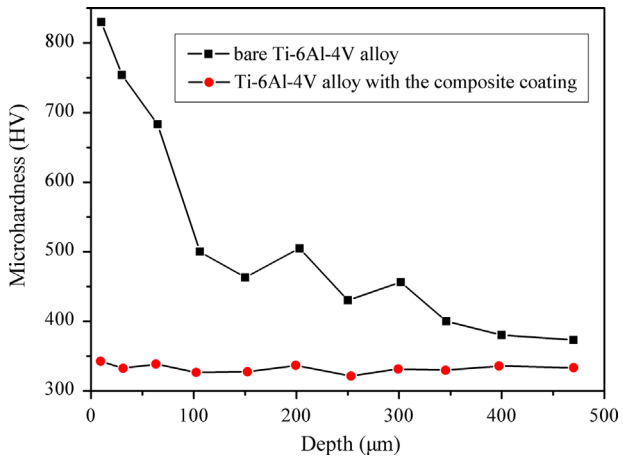

Fig. 10. Cross-sectional microhardness profile of Ti–6Al–4V alloy with and without the composite coating after oxidation for 50 h at 800 °C

Thus, a microhardness profile is capable of giving an accurate representation of oxygen diffusion in Ti alloys.

In this study, microhardness profile was obtained by plotting the measured data of microhardness against the distance from oxide scales (or coating)/substrate interface. Fig. 10 shows the cross-sectional microhardness profile of Ti–6Al–4V alloy with and without the composite coating after 50 h oxidation at 800 °C. It can be seen that the microhardness of sublayers under the oxide scales of Ti–6Al–4V alloy without coating was rather high. And the microhardness was decreasing from the oxide scales/substrate interface to the center of the alloy whose value was equal to as-casted Ti–6Al–4V ingot. It means that solid solution oxygen in Ti–6Al–4V alloy without coating was obvious, because inward diffusion of oxygen from the oxide scales (mainly composed of porous rutile TiO_2) to the bare alloys are very easy. In contrast, the cross-sectional microhardness of Ti–6Al–4V alloy with the composite coating remained stable from the coating/substrate interface to the center of the alloy. It means that the solid solution oxygen in Ti–6Al–4V alloy with composite coating was limited, which confirmed the results from the cross-sectional EDS analysis. From the above microhardness profiles, we know that the glass–amorphous silica composite coating showed good protection of Ti–6Al–4V alloy from high temperature oxidation.

4. Conclusions

A novel protective borosilicate glass–amorphous silica composite coating was successfully prepared on Ti–6Al–4V alloy at a relatively low firing temperature (850 °C). After oxidation of 50 h, mass gains of the specimens coated with the composite coating were far less than those of the uncoated ones. According to the XRD and EDS analyses, a lot of diopside and SiO_2 crystals (quartz, cristobalite) were observed in the composite coating, which are useful to slow the inward diffusion of oxygen to the substrate. The cross-sectional EDS line scanning images and the microhardness profile reveal that the solid solution oxygen in Ti–6Al–4V alloy with composite coating was insignificant. In general, the borosilicate glass–amorphous silica composite coating showed good protection of Ti–6Al–4V alloy from high temperature oxidation.

Acknowledgments

The authors are grateful for the financial support from the National Science and Technology Major Project (2012ZX 04010-081). We would also like to thank Analytical and Testing Center, Huazhong University of Science and Technology, P.R.China, for the SEM, XRD and EDS tests.

References

[1] E.A. Loria, Gamma titanium aluminides as prospective structural materials, Intermetallics 8 (2000) 1339–1345.
[2] A. Rahmel, P.J. Spencer, Thermodynamic aspects of TiAl and $TiSi_2$ oxidation: the Al–Ti–O and Si–Ti–O phase diagrams, Oxidation of Metals 35 (1991) 53–68.
[3] M. Zhu, M.S. Li, Y.L. Li, Y.C. Zhou, Influence of sol-gel derived Al_2O_3 film on the oxidation behavior of a Ti_3Al based alloy, Materials Science and Engineering A—Structural Materials 451 (2006) 177–183.
[4] H. Jiang, M. Hirohasi, Y. Lu, H. Imanari, Effect of Nb on the high temperature oxidation of Ti–(0–50 at%) Al, Scripta Materialia 46 (2002) 639–643.
[5] J.W. Fergus, Review of the effect of alloy composition on the growth rates of scales formed during oxidation of gamma titanium aluminide alloys, Materials Science and Engineering A—Structural Material 338 (2002) 108–125.
[6] H.P. Xiong, Y.H. Xie, W. Mao, Y.F. Chen, X.H. Li, Liquid-phase siliconizing and aluminizing at the surface of a Ti_3Al-based alloy and improvement in oxidation resistance, Journal of Materials Research 19 (2004) 1050–1057.
[7] H.P. Xiong, W. Mao, Y.H. Xie, W.-L. Ma, Y.F. Chen, X.H. Li, J.P. Li, Y.Y. Cheng, Liquid-phase siliconizing by Al–Si alloys at the surface of a TiAl-based alloy and improvement in oxidation resistance, Acta Materialia 52 (2004) 2605–2620.
[8] S.K. Gong, H.B. Xu, Q.H. Yu, C.G. Zhou, Oxidation behavior of TiAl/TiAl–SiC gradient coatings on gamma titanium aluminides, Surface and Coatings Technology 130 (2000) 128–132.
[9] G. Schumacher, F. Dettenwanger, M. Schutze, U. Hornauer, E. Richter, E. Wieser, Microalloying effects in the oxidation of TiAl materials, Intermetallics 7 (1999) 1113–1120.
[10] Z.W. Li, W. Gao, D. Ying, D.L. Zhang, Improved oxidation resistance of Ti with a thermal sprayed $Ti_3Al(O)$–Al_2O_3 composite coating, Scripta Materialia 48 (2003) 1649–1653.
[11] M.Z. Alam, D.K. Das, Effect of cracking in diffusion aluminide coatings on their cyclic oxidation performance on Ti-based IMI-834 alloy, Corrosion Science 51 (2009) 1405–1412.
[12] C.Z. Yu, S.L. Zhu, D. Wei, F.H. Wang, Amorphous sol–gel SiO_2 film for protection of Ti6Al4V alloy against high temperature oxidation, Surface and Coatings Technology 201 (2007) 5967–5972.
[13] X.J. Zhang, S.Y. Zhao, C.X. Gao, S.J. Wang, Amorphous sol-gel SiO_2 film for protection of an orthorhombic phase alloy against high temperature oxidation, Journal of Sol–Gel Science and Technology 49 (2009) 221–227.
[14] Z.D. Xiang, S.R. Rose, P.K. Datta, Codeposition of Al and Si to form oxidation-resistant coatings on γ-TiAl by the pack cementation process, Materials Chemistry and Physics 80 (2003) 482–489.
[15] J.K. Lee, H.N. Lee, H.K. Lee, M.H. Oh, D.M. Wee, Effects of Al-21Ti-23Cr coatings on oxidation and mechanical properties of TiAl alloy, Surface and Coatings Technology 155 (2002) 59–66.
[16] S. Sarkar, S. Datta, S. Das, D. Basu, Oxidation protection of gamma-titanium aluminide using glass-ceramic coatings, Surface and Coatings Technology 203 (2009) 1797–1805.

[17] T. Moskalewicz, F. Smeacetto, A. Czyrska-Filemonowicz, Microstructure, properties and oxidation behavior of the glass–ceramic based coating on near-α titanium alloy, Surface and Coatings Technology 203 (2009) 2249–2253.
[18] T. Moskalewicz, F. Smeacetto, G. Cempura, L.C. Ajitdoss, M. Salvo, A. Czyrska-Filemonowicz, Microstructure and properties characterisation of the double layered glass–ceramic coating on near-α titanium alloy, Surface and Coatings Technology 204 (2010) 3509–3516.
[19] W.B. Li, M.H. Chen, C. Wang, S.L. Zhu, F.H. Wang, Preparation and oxidation behavior of SiO_2–Al_2O_3-glass composite coating on Ti–47Al–2Cr–2Nb alloy, Surface and Coatings Technology 218 (2013) 30–38.
[20] D.Y. Zheng, S.L. Zhu, F.H. Wang, Oxidation and hot corrosion behavior of a novel enamel–Al_2O_3 composite coating on K38G superalloy, Surface and Coatings Technology 200 (2006) 5931–5936.
[21] M.L. Shen, S.L. Zhu, M.H. Chen, F.H. Wang, The oxidation and oxygen permeation resistance of quartz particle-reinforced aluminosilicate glass coating on titanium alloy, Journal of the American Ceramic Society 94 (2011) 2436–2441.
[22] J.H. Jean, T.K. Gupta, Crystallization kinetics of binary borosilicate glass composite, Journal of Materials Research 7 (1992) 3103–3111.
[23] G.B. Xia, L. He, D.A. Yang, Preparation and characterization of CaO–Al_2O_3–SiO_2 glass/fused silica composites for LTCC application, Journal of Alloys and Compounds 531 (2012) 70–76.
[24] A.A. El-Kheshen, M.F. Zawrah, Sinterability, microstructure and properties of glass/ceramic composites, Ceramics International 29 (2003) 251–257.
[25] M.F. Zawrah, E.M.A. Hamzawy, Effect of cristobalite formation on sinterability, microstructure and properties of glass/ceramic composites, Ceramics International 28 (2002) 123–130.
[26] H. Guleryuz, H. Cimenoglu, Oxidation of Ti–6Al–4V alloy, Journal of Alloys and Compounds 472 (2009) 241–246.
[27] C. Huang, Y.Z. Zhang, J.Y. Shena, V. Y., Thermal stability and oxidation resistance of laser clad TiVCrAlSi high entropy alloy coatings on Ti–6A–4V alloy, Surface and Coatings Technology 206 (2011) 1389–1395.
[28] H.N. Xiao, Y. Cheng, Q.Q. Yang, T. Senda, Mechanical and tribological properties of calcia–magnesia–alumina–silica–based glass–ceramics prepared by in situ crystallization, Materials Science and Engineering A—Structural Materials 423 (2006) 170–174.